Exploiting Underlying Structure for Detailed Reconstruction of an Internet-scale Event

Abhishek Kumar
Georgia Institute of Technology
akumar@cc.gatech.edu

Vern Paxson
ICSI
vern@icir.org

Nicholas Weaver
ICSI
nweaver@icsi.berkeley.edu

Abstract

Network "telescopes" that record packets sent to unused blocks of Internet address space have emerged as an important tool for observing Internet-scale events such as the spread of worms and the backscatter from flooding attacks that use spoofed source addresses. Current telescope analyses produce detailed tabulations of packet rates, victim population, and evolution over time. While such cataloging is a crucial first step in studying the telescope observations, incorporating an understanding of the underlying processes generating the observations allows us to construct detailed inferences about the broader "universe" in which the Internet-scale activity occurs, greatly enriching and deepening the analysis in the process.

In this work we apply such an analysis to the propagation of the *Witty* worm, a malicious and well-engineered worm that when released in March 2004 infected more than 12,000 hosts worldwide in 75 minutes. We show that by carefully exploiting the structure of the worm, especially its pseudo-random number generation, from limited and imperfect telescope data we can with high fidelity: extract the individual rate at which each infectee injected packets into the network *prior* to loss; correct distortions in the telescope data due to the worm's volume overwhelming the monitor; reveal the worm's inability to fully reach all of its potential victims; determine the number of disks attached to each infected machine; compute when each infectee was last booted, to sub-second accuracy; explore the "who infected whom" infection tree; uncover that the worm specifically targeted hosts at a US military base; and pinpoint *Patient Zero*, the initial point of infection, i.e., the IP address of the system the attacker used to unleash Witty.

1 Introduction

Network "telescopes" have recently emerged as important tools for observing Internet-scale events such as the spread of worms, the "backscatter" of responses from victims attacked by a flood of requests with spoofed source addresses, and incessant "background radiation" consisting of other anomalous traffic [10, 14, 15]. Telescopes record packets sent to unused blocks of Internet address space, with large ones using /8 blocks covering as much as 1/256

of the total address space. During network-wide anomalous events, such as the propagation of a worm, telescopes can collect a small yet significant slice of the worm's entire traffic. Previously, such logs of worm activity have been used to infer aggregate properties, such as the worm's infection rate (number of infected systems), the total scanning rate (number of worm copies sent per second), and the evolution of these quantities over time.

The fundamental premise of our work is that by carefully considering the underlying structure of the sources sending traffic to a telescope, we can extract a much more detailed reconstruction of such events. To this end, we analyze telescope observations of the *Witty* worm, a malicious and well-engineered[1] worm that spread worldwide in March 2004 in 75 minutes. We show that it is possible to reverse-engineer the state of each worm infectee's Pseudo-Random Number Generator (PRNG), which then allows us to recover the full set of actions undertaken by the worm. This process is greatly complicated by the worm's use of *periodic reseeding* of its PRNG, but we show it is possible to determine the new seeds, and in the process uncover detailed information about the individual hosts, including access bandwidth, up-time, and the number of physical drives attached. Our analysis also enables inferences about the network, such as shared bottlenecks and the presence or absence of losses on the path from infectees to the telescope. In addition, we uncover details unique to the propagation of the Witty worm: its failure to scan about 10% of the IP address space, the fact that it initially targeted a US military base, and the identity of *Patient Zero* — the host the worm's author used to release the worm.

Our analysis reveals systematic distortions in the data collected at telescopes and provides a means to correct this distortion, leading to more accurate estimates of quantities such as the worm's aggregate scan rate during its spread. It also identifies consequences of the specific topological placement of telescopes. In addition, detailed data about hitherto unmeasured quantities that emerges from our analysis holds promise to aid future worm simulations achieve

a degree of realism well beyond today's abstract models. The techniques developed in our study, while specific to the Witty worm, highlight the power of such analysis, and provide a template for future analysis of similar events.

We organize the paper as follows. § 2 presents background material: the operation of network telescopes and related work, the functionality of Witty, and the structure of linear-congruential PRNGs. In § 3 we provide a roadmap to the subsequent analysis. We discuss how to reverse-engineer Witty's PRNG in § 4, and then use this to estimate access bandwidth and telescope measurement distortions in § 5. § 6 presents a technique for extracting the seeds used by individual infectees upon reseeding their PRNGs, enabling measurements of each infectee's system time and number of attached disks. This section also discusses our exploration of the possible infector-infectee relationships. We discuss broader consequences of our study in § 7 and conclude in § 8.

2 Background

Network Telescopes and Related Work. Network telescopes operate by monitoring unused or mostly-unused portions of the routed Internet address space, with the largest able to record traffic sent to /8 address blocks (16.7M addresses) [10, 22]. The telescope consists of a monitoring machine that passively records all packets headed to any of the addresses in the block. Since there are few or no actual machines using these addresses, traffic headed there is generally anomalous, and often malicious, in nature. Examples of traffic observed at network telescopes include port and address scans, "backscatter" from flooding attacks, misconfigurations, and the worm packets that are of immediate interest to this work.

The first major study performed using a network telescope was the analysis of backscatter by Moore et al. [14]. This study assessed the prevalence and characteristics of spoofed-source denial-of-service (DoS) attacks and the characteristics of the victim machines. The work built on the observation that most DoS tools that spoof source addresses pick addresses without a bias towards or against the telescope's observational range. The study also inferred victim behavior by noting that the response to spoofed packets will depend on the state of the victim, particularly whether there are services running on the targeted ports.

Telescopes have been the primary tool for understanding the Internet-wide spread of previous worms, beginning with Code Red [2, 20]. Since, for a random-scanning worm, the worm is as likely to contact a telescope address as a normal address, we can extrapolate from the telescope data to compute the worm's aggregate scanning rate as it spreads. In addition, from telescope data we can see which systems were infected, thus estimate the average worm scanning rate. For high-volume sources, we can also es-

timate a source's effective bandwidth based on the rate at which its packets arrive and adjusting for the telescope's "gathering power" (portion of entire space monitored).

A variation is the *distributed telescope*, which monitors a collection of disparate address ranges to create an overall picture [1, 4]. Although some phenomena [6, 2]) scan uniformly, others either have biases in their address selection [11, 12] or simply exclude some address ranges entirely [5, 16]. Using a distributed telescope allows more opportunity to observe nonuniform phenomenon, and also reveals that, even correcting for "local preference" biases present in some forms of randomized scanning, different telescopes observe quantitatively different phenomena [4].

The biggest limitation of telescopes is their passive nature, which often limits the information we can gather. One solution useful for some studies has been *active telescopes*: changing the telescope logic to either reply with SYN-ACKs to TCP SYNs in order to capture the resulting traffic [4], or implementing a more complex state machine [15] that emulates part of the protocol. These telescopes can disambiguate scans from different worms that target the same ports by observing subsequent transactions.

In this work we take a different approach for enhancing the results of telescope measurements: augmenting traces from a telescope with a detailed analysis of the structure of the sources sending the packets. One key insight is that the PRNG used to construct "random" addresses for a worm can leak the internal state of the PRNG. By combining the telescope data with our knowledge of the PRNG, we can then determine the internal state for each copy of the worm and see how this state evolves over time.

While there have been numerous studies of Internet worms, these have either focused on detailed analysis of the worm's exact workings, beginning with analysis of the 1988 Morris Worm [7, 19], or with aggregate propagation dynamics [23, 11, 18, 20, 13]. In contrast, our analysis aims to develop a detailed understanding of the individual infected hosts and how they interacted with the network.

Datasets. We used traces from two telescopes, operated by CAIDA [10] and the University of Wisconsin [22]. Both telescopes monitor /8 blocks of IP addresses. Since each /8 contains 1/256 of all valid IPv4 addresses, these telescopes see an equivalent fraction of scan traffic addressed to random destinations picked uniformly from the 32-bit IP address space. The CAIDA telescope logs every packet it receives, while the Wisconsin telescope samples the received packets at the rate of 1/10. The CAIDA trace [17] begins at 04:45 AM UTC, running for 75 minutes and totaling 45.5M packets. The Wisconsin trace runs from 04:45 AM UTC for 75 minutes, totaling 4.1M packets.

Functionality of the Witty worm. As chronicled by Shannon and Moore [18], an Internet worm was released on Friday March 19, 2004 at approximately 8:45 PM PST (4:45 AM UTC, March 20).

1.   Seed the PRNG using system time.
2.   Send 20,000 copies of self to random destinations.
3.   Open a physical disk chosen randomly between 0 & 7.
4.   If success:
5.   Overwrite a randomly chosen block.
6.   Goto line 1.
7.   Else:
8.   Goto line 2.

Figure 1: Functionality of the Witty worm

Its payload contained the phrase "(ˆ.ˆ) insert witty message here (ˆ.ˆ)" so it came to be known as the Witty worm. The worm targeted a buffer overflow vulnerability in several Internet Security Systems (ISS) network security products.

The vulnerability exploited was a stack-based overflow in the ICQ analyzer of these security products. When they received an ICQ packet, defined as any UDP packet with *source* port 4000 and the appropriate ICQ headers, they copied the packet into a fixed-sized buffer on the stack in preparation for further analysis. The products executed this code path regardless of whether a server was listening for packets on the particular UDP destination port. In addition, some products could become infected while they *passively monitored* network links promiscuously, because they would attempt to analyze ICQ packets seen on the link even though they were not addressed to the local host.

Figure 1 shows a high-level description of the functionality of the Witty worm, as revealed by a disassembly [9]. The worm is quite compact, fitting in the first 675 bytes of a single UDP packet. Upon infecting a host, the worm first seeds its random number generator with the system time on the infected machine and then sends 20,000 copies of itself to random destinations. (These packets have a randomly selected *destination* port and a randomized amount of additional padding, but keep the source port fixed.) After sending the 20,000 packets, the worm uses a three-bit random number to pick a disk via the `open` system call. If the call returns successfully, the worm overwrites a random block on the chosen disk, reseeds its PRNG, and goes back to sending 20,000 copies of itself. Otherwise, the worm jumps directly to the send loop, continuing for another 20,000 copies, *without* reseeding its PRNG.

The LC PRNG. The Witty worm used a simple feedback-based pseudo-random number generator (PRNG) of the form known as linear congruential (LC):

$$X_{i+1} = X_i * a + b \mod m \qquad (1)$$

For a given m, picking effective values of a and b requires care lest the resulting sequences lack basic properties such as uniformity. One common parameterization is: $a = 214,013, b = 2,531,011, m = 2^{32}$.

With the above values of a, b, m, the LC PRNG generates a permutation of all the integers in $[0, m - 1]$. A key point then is that with knowledge of any X_i, all subsequent

pseudo-random numbers in the sequence can be generated by repeatedly applying Eqn 1. It is also possible to invert Eqn 1 to compute X_i if the value of X_{i+1} is known:

$$X_i = (X_{i+1} - b) * a^{-1} \mod m \qquad (2)$$

where, for $a = 214,013$, $a^{-1} = 3,115,528,533$.

Eqns 1 and 2 provide us with the machinery to generate the entire sequence of random numbers as generated by an LC PRNG, either forwards or backwards, from any arbitrary starting point on the sequence. Thus, if we can extract *any* X_i, we can compute any other X_{i+n}, given n. However, it is important to note that most uses of pseudo-random numbers, including Witty's, do *not* directly expose any X_i, but rather extract a subset of X_i's bits and intermingle them with bits from additionally generated pseudo-random numbers, as detailed below.

3 Overview of our analysis

The first step in our analysis, covered in § 4, is to develop a way to uncover the state of an infectee's PRNG. It turns out that we can do so from the observation of just a single packet sent by the infectee and seen at the telescope. (Note, however, that if recovering the state required observing consecutive packets, we would likely often still be able to do so: while the telescopes record on average only one in 256 packets transmitted by an infectee, occasionally — i.e., roughly one time out of 256 — they will happen to record consecutive packets.)

An interesting fact revealed by careful inspection of the use of pseudo-random numbers by the Witty worm is that the worm does not manage to scan the entire 32-bit address space of the Internet, in spite of using a correct implementation of the PRNG. This analysis also reveals the identity of a special host that very likely was used to start the worm.

Once we have the crucial ability to determine the state of an infectee's PRNG, we can use this state to reproduce the worm's exact actions, which then allows us to compare the resulting generated packets with the actual packets seen at the telescope. This comparison yields a wealth of information about the host generating the packets and the network the packets traversed. First, we can determine the *access bandwidth* of the infectee, i.e., the capacity of the link to which its network interface connects. In addition, given this estimate we can explore significant flaws in the telescope observations, namely packet losses due to the finite bandwidth of the telescope's inbound link. These losses cause a systematic underestimation of infectee scan rates, but we design a mechanism to correct for this bias by calibrating against our measurements of the access bandwidth. We also highlight the impact of network location of telescopes on the observations they collect (§ 5).

We next observe that choosing a random disk (line 3 of Figure 1) consumes another pseudo-random number in ad-

```
rand(){
    # Note that 32-bit integers obviate the need for
    # a modulus operation here.
    X = X * 214013 + 2531011;
    return X; }
srand(seed){ X = seed; }
main(){
    1.      srand(get_tick_count());
    2.      for (i=0; i < 20,000; ++i)
    3.              dest_ip ← rand()[0...15]||rand()[0...15];
    4.              dest_port ← rand()[0...15];
    5.              packetsize ← 768+rand()[0...8];
    6.              packetcontents ← top of stack;
    7.              sendto();
    8.      if(open(physicaldisk, rand()[13...15]))
    9.              overwrite_block(rand()[0...14]||0x4e20);
    10.             goto 1;
    11.     else goto 2; }
```

Figure 2: Pseudocode of the Witty worm

dition to those consumed by each transmitted packet. Observing such a discontinuity in the sequence of random numbers in packets from an infectee flags an attempted disk write and a potential reseeding of the infectee's PRNG. In § 6 we develop a detailed mechanism to detect the value of the seed at each such reseeding. As the seed at line 1 of Fig. 1 is set to the system time in msec since boot up, this mechanism allows us to estimate the boot time of individual infectees just by looking at the sequence of occasional packets received at the telescope. Once we know the PRNG's seed, we can precisely determine the random numbers it generates to synthesize the next 20,000 packets, and also the three-bit random number it uses next time to pick a physical disk to open. We can additionally deduce the success or failure of this open system call by whether the PRNG state for subsequent packets from the same infectee follow in the same series or not. Thus, this analysis reveals the number of physical disks on the infectee.

Lastly, knowledge of the seeds also provides access to the complete list of packets sent by the infectee. This allows us to infer infector-infectee relationships during the worm's propagation.

4   Analysis of Witty's PRNG

The first step in our analysis is to examine a disassembly of the binary code of the Witty worm [9]. Security researchers typically publish such disassemblies immediately after the release of a worm in an attempt to understand the worm's behavior and devise suitable countermeasures. Figure 2 shows the detailed pseudocode of the Witty worm as derived from one such disassembly [9]. The rand() function implements the Linear Congruential PRNG as discussed in § 2. In the rest of this section, we use the knowledge of the pseudocode to develop a technique for deducing the state of the PRNG at an infectee from any *single* packet sent by it. We also describe how as a consequence of the specific

manner in which Witty uses the pseudo-random numbers, the worm fails to scan the entire IP address space, and also reveals the identity of *Patient Zero*.

Breaking the state of the PRNG at the infectee. The Witty worm constructs "random"destination IP addresses by concatenating the top 16 bits of two consecutive pseudo random numbers generated by its PRNG. In our notation, $X_{[0\cdots15]}$ represents the top 16 bits of the 32 bit number X, with bit 0 being the most significant. The destination port number is constructed by taking the top 16 bits of the next (third) random number. The packet size[2] itself is chosen by adding the top 9 bits of a fourth random number to 768. Thus, each packet sent by the Witty worm contains bits from four consecutive random numbers, corresponding to lines 3,4 and 5 in Fig. 2. If all 32 bits of any of these numbers were known, it would completely specify the state of the PRNG. But since only some of the bits from each of these numbers is known, we need to design a mechanism to retrieve all 32 bits of one of these numbers from the partial information contained in each packet.

To do so, if the first call to rand() returns X_i, then:

$$dest\_ip = X_{i,[0\cdots15]}||X_{i+1,[0\cdots15]}$$
$$dest\_port = X_{i+2,[0\cdots15]}$$

where $||$ is the concatenation operation. Now, we know that X_i and X_{i+1} are related by Eqn 1, and so are X_{i+1} and X_{i+2}. Furthermore, there are only 65,536 (2^{16}) possibilities for the lower 16 bits of X_i, and only one of them is such that when used with $X_{i,[0\cdots15]}$ (available from the packet) the next two numbers generated by Eqn 1 have the same top 16 bits as $X_{i+1,[0\cdots15]}$ and $X_{i+2,[0\cdots15]}$, which are also observed in the received packet. In other words, there is only one 16-bit number Y that satisfies the following two equations simultaneously:

$$X_{i+1,[0\cdots15]} = (X_{i,[0\cdots15]}||Y * a \mod m)_{[0\cdots15]}$$

$$X_{i+2,[0\cdots15]} = ((X_{i,[0\cdots15]}||Y*a \mod m)*a \mod m)_{[0\cdots}$$

For each of the 2^{16} possible values of Y, verifying the first equality takes one addition and one multiplication.[3] Thus trying all 2^{16} possibilities is fairly inexpensive. For the small number of possible values of Y that satisfy the first equation, we try the second equation, and the value Y^* that satisfies both the equations gives us the lower sixteen bits of X_i (i.e., $X_{i,[16\cdots31]} = Y^*$). In our experiments, we found that on the average about two of the 2^{16} possible values satisfy the first equation, but there was always a unique value of Y^* that satisfied both the equations.

Why Witty fails to scan the entire address space. The first and somewhat surprising outcome from investigating how Witty constructs random destination addresses is the observation that Witty fails to scan the entire IP address space. This means that, while Witty spread at a very high

speed (infecting 12,000 hosts in 75 minutes), due to a subtle error in its use of pseudo-random numbers about 10% of vulnerable hosts were never infected with the worm.

To understand this flaw in full detail, we first visit the motivation for the use of only the top 16 bits of the 32 bit results returned by Witty's LC PRNG. This was recommended by Knuth [8], who showed that the high order bits are "more random" than the lower order bits returned by the LC PRNG. Indeed, for this very reason, several implementations of the rand() function, including the default C library of Windows and SunOS, return a 15 bit number, even though their underlying LC PRNG uses the same parameters as the Witty worm and produces 32 bit numbers.

However, this advice was taken out of context by the author of the Witty worm. Knuth's advice applies when *uniform randomness* is the desired property, and is valid only when a small number of random bits are needed. For a worm trying to maximize the number of infected hosts, one reason for using random numbers while selecting destinations is to avoid detection by intrusion detection systems that readily detect sequential scans. A second reason is to maintain independence between the portions of the address-space scanned by individual infectees. Neither of these reasons actually requires the kind of "good randomness" provided by following Knuth's advice of picking only the higher order bits.

As discussed in § 2, for specific values of the parameters a, b and m, the LC PRNG is a *permutation* PRNG that generates a permutation of all integers in the range 0 to $m - 1$. By the above definition, if the Witty worm were to use the entire 32 bits of a single output of its LC PRNG as a destination address, it would eventually generate each possible 32-bit number, hence successfully scanning the entire IP address space. (This would also of course make it trivial to recover the PRNG state.) However, the worm's author chose to use the concatenation of the top 16 bits of two consecutive random numbers from its PRNG. With this action, the guarantee that each possible 32-bit number will be generated is lost. In other words, there is no certainty that the set of 32-bit numbers generated in this manner will include all integers in the set $[0, 2^{32} - 1]$.

We enumerated Witty's entire "orbit" and found that there are 431,554,560 32-bit numbers that can never be generated. This corresponds to 10.05% of the IP address space that was never scanned by Witty. On further investigation, we found these unscanned addresses to be fairly uniformly distributed over the 32-bit address space of IPv4. Hence, it is reasonable to assume that approximately the same fraction of the *populated* IP address space was missed by Witty. In other words, even though the portions of IP address space that are actually used (populated) are highly clustered, because the addresses that Witty misses are uniformly distributed over the space of 32-bit integers, it missed roughly the same fraction of address among the
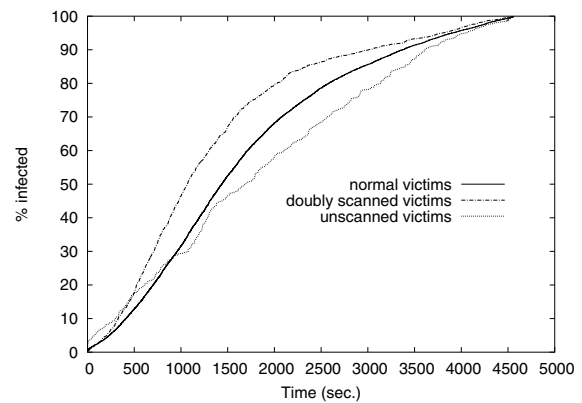

Figure 3: Growth curves for victims whose addresses were scanned once per orbit, twice per orbit, or not at all.

set of IP addresses in actual use.

Observing that Witty does not visit some addresses at all, one might ask whether it visits some addresses more frequently than others. Stated more formally, given that the period of Witty's PRNG is 2^{32}, it must generate 2^{32} unique (X_i, X_{i+1}) pairs, from which it constructs 2^{32} 32-bit destination IP addresses. Since this set of 2^{32} addresses does not contain the 431,554,560 addresses missed by Witty, it must contain some repetitions. What is the nature of these repetitions? Interestingly, there are exactly 431,554,560 *other* 32-bit numbers that occur twice in this set, and no 32-bit numbers that occur three or more times. This is surprising because, in general, in lieu of the 431,554,560 missed numbers, one would expect some number to be visited twice, others to be visited thrice and so on. However, the peculiar structure of the sequence generated by the LC PRNG with specific parameter values created the situation that exactly the same number of other addresses were visited twice and none were visited more frequently.

During the first 75 minutes of the release of the Witty worm, the CAIDA telescope saw 12,451 unique IP addresses as infected. Following the above discussion, we classified these addresses into three classes. There were 10,638 (85.4%) addresses that were scanned just once in an orbit, i.e., addresses that experienced a normal scan rate. Another 1,409 addresses (11.3%) were scanned twice in an orbit, hence experiencing twice the normal growth rate. A third class of 404 (3.2%) addresses belonged to the set of addresses *never* scanned by the worm. At first blush one might wonder how these latter could possibly appear, but we can explain their presence as reflecting inclusion in an initial "hit list" (see below), operating in promiscuous mode, or aliasing due to multi-homing, NAT or DHCP.

Figure 3 compares the growth curves for the three classes of addresses. Notice how the worm spreads faster among the population of machines that experience double the normal scan rate. 1,000 sec from its release, Witty had infected

half of the doubly-scanned addresses that it would infect in the first 75 min. On the other hand, in the normally-scanned population, it had only managed to infect about a third of the total victims that it would infect in 75 min. Later in the hour, the curve for the doubly-scanned addresses is flatter than that for the normally-scanned ones, indicating that most of the victims in the doubly-scanned population were already infected at that point.

The curve for infectees whose source address was *never* scanned by Witty is particularly interesting. Twelve of the never-scanned systems appear in the first 10 seconds of the worm's propagation, very strongly suggesting that they are part of an initial hit-list. This explains the early jump in the plot: it's not that such machines are overrepresented in the hit-list, rather they are underrepresented in the total infected population, making the hit-list propagation more significant for this population.

Another class of never-scanned infectees are those passively monitoring a network link. Because these operate in promiscuous mode, their "cross section" for becoming infected is magnified by the address range routed over the link. On average, these then will become infected much more rapidly than normal over even doubly-scanned hosts. We speculate that these infectees constitute the remainder of the early rise in the appearance of never-scanned systems. Later, the growth rate of the never-scanned systems substantially slows, lagging even the single-scanned addresses. Likely these remaining systems reflect infrequent aliasing due to multihoming, NAT, or DHCP.

Identifying Patient Zero. Along with "Can all addresses be reached by scans?", another question to ask is "Do all sources indeed travel on the PRNG orbit?" Surprisingly, the answer is No. There is a single Witty source that consistently fails to follow the orbit. Further inspection reveals that the source *(i)* always generates addresses of the form $A.B.A.B$ rather than $A.B.C.D$, *(ii)* does not randomize the packet size, and *(iii)* is present near the very beginning of the trace, but not before the worm itself begins propagating. That the source fails to follow the orbit clearly indicates that it is running *different* code than do all the others; that it does not appear prior to the worm's onset indicates that it is not a background scanner from earlier testing or probing (indeed, it sends valid Witty packets which could trigger an infection); and that it sends to sources of a limited form suggests a bug in its structure that went unnoticed due to a lack of testing of this particular Witty variant.

We argue that these peculiarities add up to a strong likelihood that this unique host reflects *Patient Zero*, the system used by the attacker to seed the worm initially. Patient Zero was not running the complete Witty worm but rather a (not fully tested) tool used to launch the worm. To our knowledge, this represents the first time that Patient Zero has been identified for a major worm outbreak.[4] We have conveyed the host's IP address (which corresponds to a Eu-

ropean retail ISP) to law enforcement.

If all Patient Zero did was send packets of the form $A.B.A.B$ as we observed, then the worm would not have spread, as we detected no infectees with such addresses. However, as developed both above in discussing Figure 3 and later in § 6, the evidence is compelling that Patient Zero first worked through a "hit list" of known-vulnerable hosts before settling into its ineffective scanning pattern.

5 Bandwidth measurements

An important use of network telescopes lies in inferring the scanning rate of a worm by extrapolating from the observed packets rates from individual sources. In this section, we develop a technique based on our analysis of Witty's PRNG to estimate the access bandwidth of individual infectees. We then identify an obvious source of systematic error in extrapolation based techniques, namely the bottleneck at the telescope's inbound link, and suggest a solution to correct this error.

Estimating Infectee Access Bandwidth. The access bandwidth of the population of infected machines is an important variable in the dynamics of the spread of a worm. Using the ability to deduce the state of the PRNG at an infectee, we can infer this quantity, as follows. The Witty worm uses the `sendto` system call, which is a *blocking* system call by default in Windows: the call will not return till the packet has been successfully written to the buffer of the network interface. Thus, no worm packets are dropped either in the kernel or in the buffer of the network interface. But the network interface can clear out its buffer at most at its transmission speed. Thus, the use of blocking system calls indirectly clocks the rate of packet generation of the Witty worm to match the maximum transmission bandwidth of the network interface on the infectee.

We estimate the access bandwidth of an infectee as follows. Let P_i and P_j be two packets from the same infectee, received at the telescope at time t_i and t_j respectively. Using the mechanism developed in § 4 we can deduce X_i and X_j, the state of the PRNG at the sender when the two respective packets were sent. Now, we can simulate the LC PRNG with an initial state of X_i and repeatedly apply Eqn 1 till the state advances to X_j. The number of times Eqn 1 is applied to get from X_i to X_j is the value of $j - i$. Since it takes 4 cranks of the PRNG to construct each packet (lines 3–5, in Fig. 2), the total number of packets between P_i and P_j is $(j - i)/4$. Thus the access bandwidth of the infectee is approximately $average\_packetsize * (j-i)/4 * 1/(t_j - t_i)$. While we can compute it more precisely, since reproducing the PRNG sequence lets us extract the exact size of each intervening packet sent, for convenience we will often use the average payload size (1070 bytes including UDP, IP and Ethernet headers). Thus, the transmission rate can be computed as
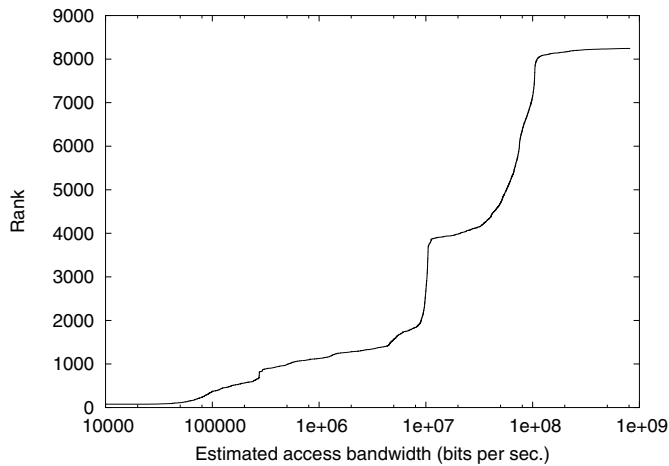
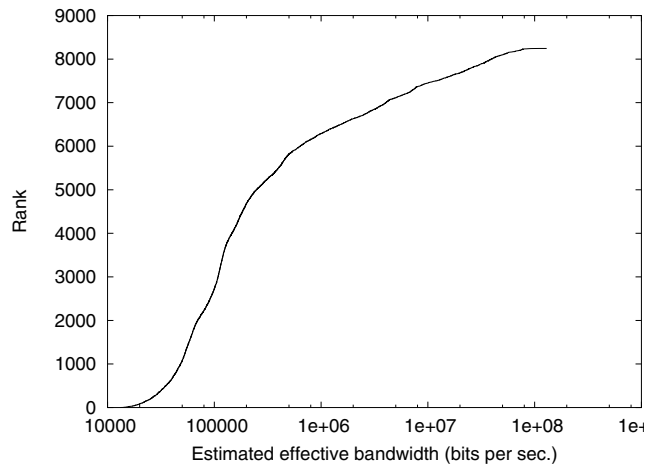Figure 4: Access bandwidth of Witty infectees estimated using our technique.

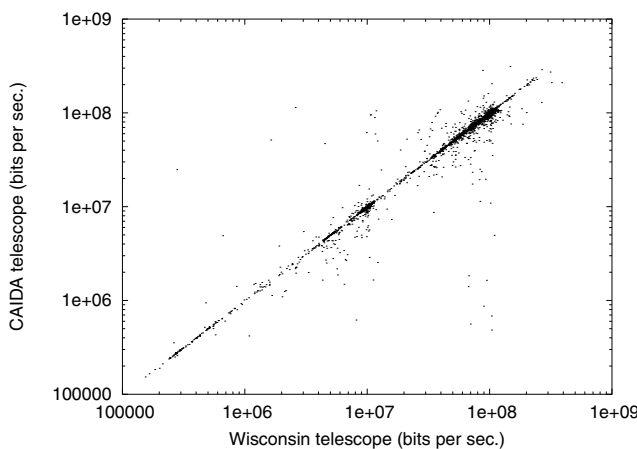Figure 6: Effective bandwidth of Witty infectees.

Figure 5: Comparison of estimated access bandwidth using data from two telescopes.

$$\frac{(j-i)*1070*8}{4(t_j-t_i)} = 2140\frac{j-i}{t_j-t_i} \text{ bits per second.}$$

Figure 4 shows the estimates of access bandwidth of infectees[5] that appeared at the CAIDA telescope from 05:01 AM to 06:01 AM UTC (i.e., starting about 15 min after the worm's release). The x-axis shows the estimated access bandwidth in bps on log scale, and the y-axis shows the rank of each infectee in increasing order. It is notable in the figure that about 25% of the infectees have an access bandwidth of 10 Mbps while about 50% have a bandwidth of 100 Mbps. This corresponds well with the popular workstation configurations connected to enterprise LANs (a likely description of a machine running the ISS software vulnerable to Witty), or to home machines that include an Ethernet segment connecting to a cable or DSL modem.

We use the second set of observations, collected independently at the Wisconsin telescope (located far from the CAIDA telescope), to test the accuracy of our estimation, as shown in Figure 5. Each point in the scatter plot represents a source observed in both datasets, with its x and y coordinates reflecting the estimates from the Wisconsin and CAIDA observations, respectively. Most points are located very close to the $y = x$ line, signifying close agreement. The small number of points (about 1%) that are significantly far from the $y = x$ line merit further investigation. We believe these reflect NAT effects invalidating our inferences concerning the amount of data a "single" source sends during a given interval.

Extrapolation-based estimation of effective bandwidth. Previous analyses of telescope data (e.g., [18]) used a simple extrapolation-based technique to estimate the bandwidth of the infectees. The reasoning is that given a telescope captures a /8 address block, it should see about 1/256 of the worm traffic. Thus, after computing the packets per second from individual infectees, one can extrapolate this observation by multiplying by 256 to estimate the total packets sent by the infectee in the corresponding period. Multiplying again by the average packet size (1070 bytes) gives the extrapolation-based estimate of the bandwidth of the infectee. Notice that this technique is not measuring the *access* bandwidth of the infectee, but rather the *effective* bandwidth, i.e., the rate at which packets from the infectee are actually delivered across the network.

Figure 6 shows the estimated bandwidth of the same population of infectees, computed using the extrapolation technique. The effective bandwidth so computed is significantly lower than the access bandwidth of the entire population. To explore this further, we draw a scatter-plot of the estimates using both techniques in Fig. 7. Each point corresponds to the PRNG-estimated access bandwidth (x axis) and extrapolation-based effective bandwidth (y axis). The modes at 10 and 100 Mbps in Fig. 4 manifest as clusters of points near the lines $x = 10^7$ and $x = 10^8$, re-
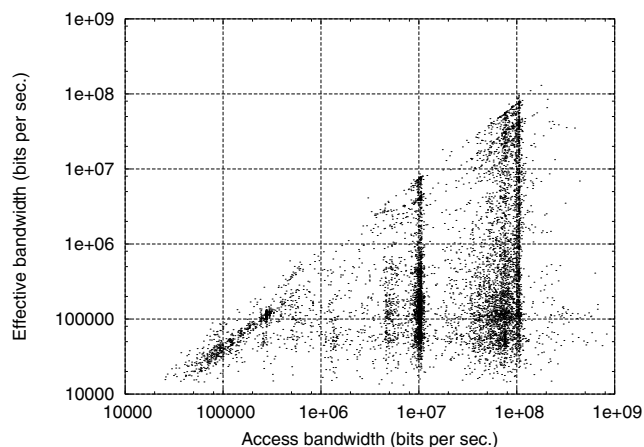
Figure 7: Scatter-plot of estimated bandwidth using the two techniques.

Figure 8: Aggregate worm traffic in pkts/sec as actually logged at the telescope.

spectively. As expected, all points lie below the diagonal, indicating that the effective bandwidth never exceeds the access bandwidth, and is often lower by a significant factor. During infections of bandwidth-limited worms, i.e., worms such as Witty that send fast enough to potentially consume all of the infectee's bandwidth, mild to severe congestion, engendering moderate to significant packet losses, is likely to occur in various portions of the network.

Another possible reason for observing diminished effective bandwidth is multiple infectees sharing a bottleneck, most likely because they reside within the same subnet and contend for a common uplink. Indeed, this effect is noticeable at /16 granularity. That is, sources exhibiting very high loss rates (effective bandwidth < 10% of access bandwidth) are significantly more likely to reside in /16 prefixes that include other infectees, than are sources with lower loss rates (effective > 50% access). For example, only 20% of the sources exhibiting high loss reside alone in their own /16, while 50% of those exhibiting lower loss do.

Telescope Fidelity. An important but easy-to-miss feature of Fig. 7 is that the upper envelope of the points is *not* the line $y = x$ but rather $y \approx 0.7x$, which shows up as the upper envelope of the scatter plot lying parallel to, but slightly below, the diagonal. This implies either a loss rate of nearly 30% for even the best connected infectees, or a systematic error in the observations. Further investigation immediately reveals the cause of the systematic error, namely congestion on the inbound link of the telescope. Figure 8 plots the packets received during one-second windows against time from the release of the worm. There is a clear ramp-up in aggregate packet rate during the initial 800 seconds after which it settles at approximately 11,000 pkts/sec. For an average packet size of 1,070 bytes, a rate of 11,000 pkts/sec corresponds to 95 Mbps, nearly the entire inbound bandwidth of 100 Mbps of the CAIDA
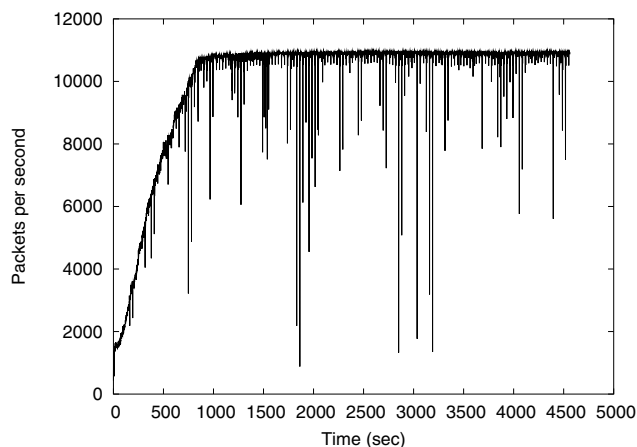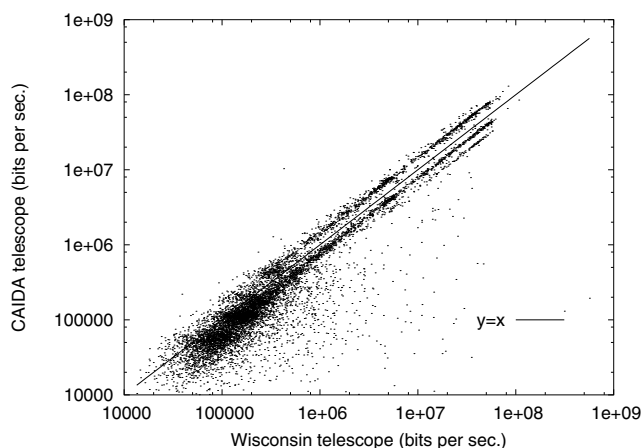

Figure 9: Comparison of effective bandwidth as estimated at the two telescopes.

telescope at that time.[6]

Fig. 8 suggests that the telescope may not have suffered any significant losses in the first 800 seconds of the spread of the worm. We verified this using a scatter-plot similar to Fig. 7, but only for data collected in the first 600 seconds of the infection. In that plot, omitted here due to lack of space, the upper envelope is indeed $y = x$, indicating that the best connected infectees were able to send packets unimpeded across the Internet, as fast as they could generate them.

A key point here is that our ability to determine access bandwidth allows us to *quantify* the 30% distortion[7] at the telescope due to its limited capacity. In the absence of this fine-grained analysis, we would have been limited to noting that the telescope saturated, but without knowing how much we were therefore missing.

Figure 9 shows a scatter-plot of the estimates of effective bandwidth as estimated from the observations at the

CAIDA ≥ Wisc.*1.05		Wisc. ≥CAIDA*1.05	
# Domains	TLD	# Domains	TLD
53	.edu	64	.net
17	.net	35	.com
7	.jp	9	.edu
5	.nl	7	.cn
5	.com	5	.nl
5	.ca	4	.ru
3	.tw	3	.jp
3	.gov	3	.gov
25	*other*	19	*other*

Table 1: Domains with divergent estimates of effective bandwidth.

two telescopes. We might expect these to agree, with most points lying close to the $y = x$ line, other than perhaps for differing losses due to saturation at the telescopes themselves, for which we can correct. Instead, we find two major clusters that lie approximately along $y = 1.4x$ and $y = x/1.2$. These lie parallel to the $y = x$ line due to the logscale on both axes. We see a smaller third cluster below the $y = x$ line, too. These clusters indicate systematic divergence in the telescope observations, and *not* simply a case of one telescope suffering more saturation losses than the other, which would result in a *single* line either above or below $y = x$.

To analyze this effect, we took all of the sources with an effective bandwidth estimate from both telescopes of more than 10 Mbps. We resolved each of these to domain names via reverse DNS lookups, taking the domain of the responding nameserver if no PTR record existed. We then selected a representative for each of the unique second-level domains present among these, totaling 900. Of these, only 29 domains had estimates at the two telescopes that agreed within 5% after correcting for systematic telescope loss. For 423 domains, the corrected estimates at CAIDA exceeded those at Wisconsin by 5% or more, while the remaining 448 had estimates at Wisconsin that exceeded CAIDA's by 5% or more.

Table 1 lists the top-level domains for the unique second-level domains that demonstrated ≥ 5% divergence in estimated effective bandwidth. Owing to its connection to Internet-2, the CAIDA telescope saw packets from .edu with significantly fewer losses than the Wisconsin telescope, which in turn had a better reachability from hosts in the .net and .com domains. Clearly, telescopes are not "ideal"devices, with perfectly balanced connectivity to the rest of the Internet, as implicitly assumed by extrapolation-based techniques. Rather, what a telescope sees during an event of large enough volume to saturate high-capacity Internet links is dictated by its specific location on the Internet topology. This finding complements that of [4], which found that the (low-volume) background radiation seen at different telescopes likewise varies significantly with loca-

tion, beyond just the bias of some malware to prefer nearby addresses when scanning.

6 Deducing the seed

Cracking the seeds — System uptime. We now describe how we can use the telescope observations to deduce the exact values of the seeds used to (re)initialize Witty's PRNG. Recall from Fig. 2 that the Witty worm attempts to open a disk after every 20,000 packets, and re-seeds its PRNG on success. To get a seed with reasonable local entropy, Witty uses the value returned by the Get_Tick_Count system call, a counter set to zero at boot time and incremented every millisecond.

In § 4 we have developed the capability to reverse-engineer the state of the PRNG at an infectee from packets received at the telescope. Additionally, Eqns 1 and 2 give us the ability to crank the PRNG forwards and backwards to determine the state at preceding and successive packets. Now, for a packet received at the telescope, if we could identify the precise number of calls to the function rand between the reseeding of the PRNG and the generation of the packet, simply cranking the PRNG backwards the same number of steps would reveal the value of the seed. The difficulty here is that for a given packet we do *not* know which "generation"it is since the PRNG was seeded. (Recall that we only see a few of every thousand packets sent.) We thus have to resort to a more circuitous technique.

We split the description of our approach into two parts: a technique for identifying a small range in the orbit (permutation sequence) of the PRNG where the seed must lie, and a geometric algorithm for finding the seeds from this candidate set.

Identifying a limited range within which the seed must lie. Figure 10 shows a graphical view of our technique for restricting the range where the seed can potentially lie. Figure 10(a) shows the sequence of packets as generated at the infectee. The straight line at the top of the figure represents the permutation-space of the PRNG, i.e., the sequence of numbers $X_0, X_1, \cdots, X_{2^{32}-1}$ as generated by the PRNG. The second horizontal line in the middle of the figure represents a small section of this sequence, blown-up to show the individual numbers in the sequence as ticks on the horizontal line. Notice how each packet consumes exactly four random numbers, represented by the small arcs straddling four ticks.

Only a small fraction of packets generated at the infectee reach the telescope. Figure 10(b) shows four such packets. By cranking forward from the PRNG's state at the first packet until the PRNG reaches the state at the second packet, we can determine the precise number of calls to the rand function in the intervening period. In other words, if we start from the state corresponding to the first packet and apply Eqn 1 repeatedly, we will eventually (though see
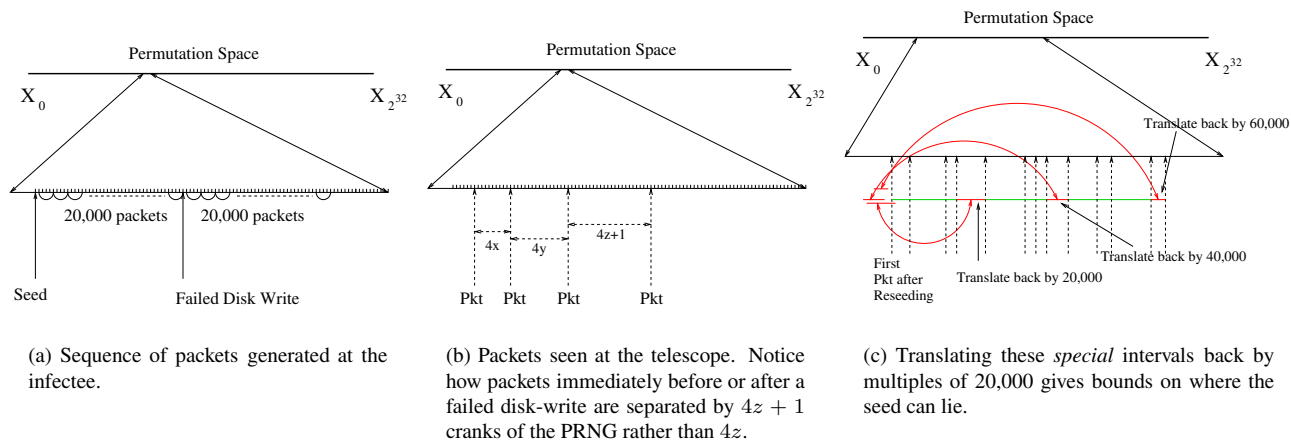
(a) Sequence of packets generated at the infectee.

(b) Packets seen at the telescope. Notice how packets immediately before or after a failed disk-write are separated by $4z + 1$ cranks of the PRNG rather than $4z$.

(c) Translating these *special* intervals back by multiples of 20,000 gives bounds on where the seed can lie.

Figure 10: Restricting the range where potential seeds can lie.

below) reach the state corresponding to the second packet, and counting the number of times Eqn 1 was applied gives us the precise number of random numbers generated between the departure of these two packets from the infectee. Note that since each packet consumes four random numbers (the inner loop of lines 2–7 in Fig. 2), the number of random numbers will be a multiple of four.

However, sometimes we find the state for a packet received at the telescope does *not* lie within a reasonable number of steps (300,000 calls to the PRNG) from the state of the preceding packet from the same infectee. This signifies a potential reseeding event: the worm finished its batch of 20,000 packets and attempted to open a disk to overwrite a random block. Recall that there are two possibilities: the random disk picked by the worm exists, in which case it overwrites a random block and (regardless of the success of that attempted overwrite) reseeds the PRNG, jumping to an arbitrary location in the permutation space (control flowing through lines 8→9→10→1→2 in Fig. 2); or the disk does not exist, in which case the worm continues for another 20,000 packets *without* reseeding (control flowing through lines 8→11→2 in Fig. 2). Note that *in either case* the worm consumes a random number in picking the disk.

Thus, every time the worm finishes a batch of 20,000 packets, we will see a discontinuity in the usual pattern of $4z$ random numbers between observed packets. We will instead either find that the packets correspond to $4z + 1$ random numbers between them (disk open failed, no reseeding); or that they have no discernible correspondence (disk open succeeded, PRNG reseeded and now generating from a different point in the permutation space).

This gives us the ability to identify intervals within which either failed disk writes occurred, or reseeding events occurred. Consider the interval straddled by the first failed disk write after a successful reseeding. Since the worm attempts disk writes every 20,000 packets, this interval translated back by 20,000 packets (80,000 calls to the

PRNG) must straddle the seed. In other words, the beginning of this special interval must lie no more than 20,000 packets away from the reseeding event, and its end must lie no less than that distance away. This gives us upper *and* lower bounds on where the reseeding must have occurred. A key point is that these bounds are *in addition* to the bounds we obtain from observing that the worm reseeded. Similarly, if the worm fails at its next disk write attempt too, the interval straddling *that* failed write, when translated backwards by 40,000 packets (160,000 calls to the PRNG), gives us another pair of lower and upper bounds on where the seed must lie. Continuing this chain of reasoning, we can find multiple upper and lower bounds. We then take the *max* of all lower bounds and the *min* of all upper bounds to get the tightest bounds, per Figure 10(c).

A geometric algorithm to detect the seeds. Given this procedure, for each reseeding event we can find a limited range of potential in the permutation space wherein the new seed must lie. (I.e., the possible seeds are consecutive over a range in the permutation space of the consecutive 32-bit random numbers as produced by the LC PRNG; they are *not* consecutive 32-bit integers.) Note, however, that this may still include hundreds or thousands of candidates, scattered over the full range of 32-bit integers.

Which is the correct one? We proceed by leveraging two key points: *(i)* for most sources we can find numerous reseeding events, and *(ii)* the actual seeds at each event are strongly related to one another by the *amount of time* that elapsed between the events, since the seeds are *clock readings*. Regarding this second point, recall that the seeds are read off a counter that tracks the number of milliseconds since system boot-up. Clearly, this value increases linearly with time. So if we observe two reseeding events with timestamps (at the telescope) of t_1 and t_2, with corresponding seeds S_1 and S_2, then because clocks progress linearly with time, $(S_2 - S_1) \approx (t_2 - t_1)$. In other words, if the infectee reseeded twice, then the value of the seeds
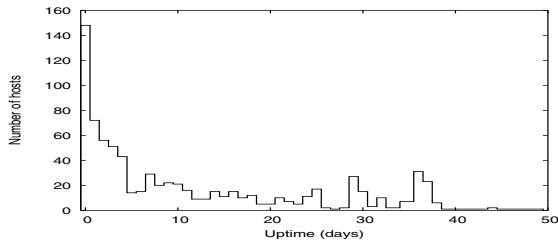
Figure 11: Number of infectees with a system uptime of the given number of days.

must differ by approximately the same amount as the difference in milliseconds in the timestamps of the two packets seen immediately after these reseedings at the telescope. Extending this reasoning to k reseeding events, we get $(S_j - S_i) \approx (t_j - t_i), \forall i, j : 1 \leq i, j \leq k$. This implies that the k points (t_i, S_i) should (approximately) lie along a straight line with slope 1 (angle of $45°$) when plotting potential seed value against time.

We now describe a geometric algorithm to detect such a set of points in a 2-dimensional plane. The key observation is that when k points lie close to a straight line of a given slope, then looking from any one of these points along that slope, the remaining points should appear clustered in a very narrow band. More formally, if we project an angular beam of width δ from any one of these points, then the remaining points should lie within the beam, for reasonably small values of δ. On the other hand, other, randomly scattered points on the plane will see a very small number of other points in the beam projected from them.

The algorithm follows directly from this observation. It proceeds in iterations. Within an iteration, we project a beam of width $\delta = \arctan 0.1 \approx 0.1$ along the $45°$ line from each point in the plane. The point is assigned a score equal to the number of other points that lie in its beam. Actual seeds are likely to get a high score because they would all lie roughly along a $45°$ line. At the end of the iteration, all points with a score smaller than some threshold (say $k/2$) are discarded. Repeating this process in subsequent iterations quickly eliminates all but the k seeds, which keep supporting high scores for each other in all iterations.

We find this algorithm highly effective given enough reseeding events. Figure 11 presents the results of the computation of system uptime of 784 machines in the infectee population. These infectees were chosen from the set that contributed enough packets to allow us to use our mechanism for estimating the seed. Since the counter used by Witty to reseed its PRNG is only 32 bits wide, it will wrap-around every 2^{32} milliseconds, which is approximately 49.7 days. The results could potentially be distorted due to this effect (but see below).

There is a clear domination of short-lived machines, with approximately 47% having uptimes of less than five days. On the other hand, there are just five machines that had an

uptime of more than 40 days. The sharp drop-off above 40 days leads us to conclude that the effects due to the wrapping-around of the counter are negligible.

The highest number of machines were booted on the same day as the spread of the worm. There are prominent troughs during the weekends — recall that the worm was released on a Friday evening Pacific Time, so the nearest weekend had passed 5 days previously — and heightened activity during the working days.

One feature that stands out is the presence of two modes, one at 29 days and the second at 36/37 days. On further investigation, we found that the machines in the first mode all belonged to a set of 135 infectees from the same /16 address block, and traceroutes revealed they were situated at a single US military installation. Similarly, machines in the second mode belonged to a group of 81 infectees from another /16 address block, belonging to an educational institution. However, while machines in the second group appeared at the telescope one-by-one throughout the infection period, 110 of the 135 machines in the first group appeared at the telescope within 10 seconds of Witty's onset. Since such a fast spread is not feasible by random scanning of the address space, the authors of [18] concluded that these machines were either part of a hit-list or were already compromised and under the control of the attacker. Because we can fit the actions of these infectees with running the full Witty code, including PRNG reseeding patterns that match the process of overwriting disk blocks, this provides evidence that these machines were not specially controlled by the attacker (unlike the *Patient Zero* machine), and thus we conclude that they likely constitute a hit-list. (We investigated an alternate explanation that instead these machines were passively monitoring large address regions and hence were infected much more quickly, but can discount this possibility because a "lineage" analysis reveals that a significant number of the machines did not receive any infection packets on even their entire local /16 prior to their own scanning activity arriving at the telescope. Additionally, these systems' IP addresses also suggest local monitors, rather than a collection of global monitors on a large address space.) Returning then to the fact that these machines were all rebooted exactly 29 days before the onset of the worm, we speculate that the reboot was due to a facility-wide system upgrade; perhaps the installation of system software such as Microsoft updates (a critical update had been released on Feb. 10, about 10 days before the simultaneous system reboots), or perhaps the installation of the vulnerable ISS products themselves. We might then speculate that the attacker *knew* about the ISS installation at the site (thus enabling them to construct a hit-list), which, along with the attacker's rapid construction of the worm indicating they likely knew about the vulnerability in advance [21], suggests that the attacker was an ISS "insider."

Number of disks. Once we can recover the seed used at

Number of Disks	1	2	3	4	5	6	7
Number of Infectees	52	32	12	2	2	0	0

Table 2: Disk counts of 100 infectees.

the beginning of a sequence of packets, we can use its value as an anchor to mark off the precise subsequent actions of the worm. Recall from Fig. 2 that the worm generates exactly 20,000 packets in its inner loop, using 80,000 random numbers in the process. After exiting the inner loop, the worm uses three bits from the next random number to decide which physical disk it will attempt to open. Starting from the seed, this is exactly the 80,001th number in the sequence generated by the PRNG. Thus, knowledge of the seed tells us exactly which disk the worm attempts to open. Furthermore, as discussed above we can tell whether this attempt succeeded based on whether the worm reseeds after the attempt. We can therefore estimate the number of disks on the infectee, based on which of the attempts for drives in the range 0 to 7 lead to a successful return from the open system call. Table 2 shows the number of disks for 100 infectees, calculated using this approach. The majority of infectees had just one or two disks, while we find a few with up to five disks. Since the installation of end-system fire wall software was a prerequisite for infection by Witty, the infectee population is more likely to contain production servers with multiple disks.

Exploration of infection graph. Knowledge of the precise seeds allows us to reconstruct the complete list of packets sent by each infectee. Additionally, the large size of our telescope allows us to detect an infectee within the first few seconds (few hundred packets) of its infection. Therefore if an infectee is first seen at a time T, we can inspect the list of packets sent by all other infectees active within a short preceding interval, say $(T - 10 \text{ sec}, T)$, to see which sent a packet to the new infectee, and thus is the infectee's likely "infector" to select the most likely "infector".

The probability of more than one infectee sending a worm packet to the same new infectee at the time of its infection is quite low. With about 11,000 pkts/sec seen at a telescope with 1/256 of the entire Internet address space, and suffering 30% losses due to congestion (§ 5), the aggregate scanning rate of the worm comes out to around $256 \cdot 11,000/0.7 \approx 4 \cdot 10^6$ pkts/sec. With more than $4 \cdot 10^9$ addresses to scan, the probability that more than one infectee scans the same address within the same 10 second interval is around 1%.

Figure 12 shows scan packets from infected sources that targeted other infectees seen at the telescope. The x-coordinate gives t_{scan}, the packet's estimated sending time, and the y-coordinate gives the difference between $t_{\text{infection}}$, the time when the target infectee first appeared at the telescope, and t_{scan}. A small positive value of $t_{\text{infection}} - t_{\text{scan}}$ raises strong suspicions that the given scan packet is re-
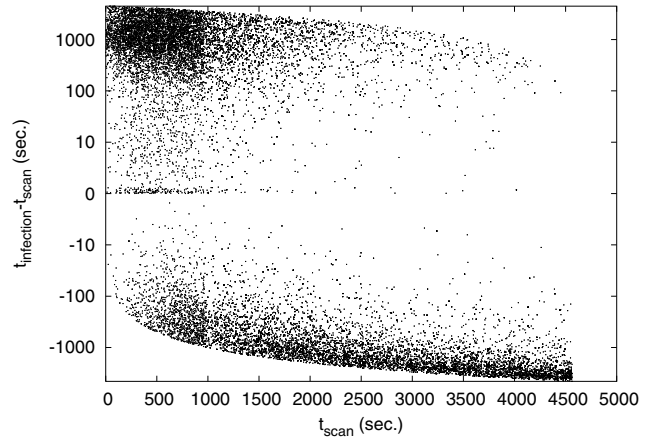

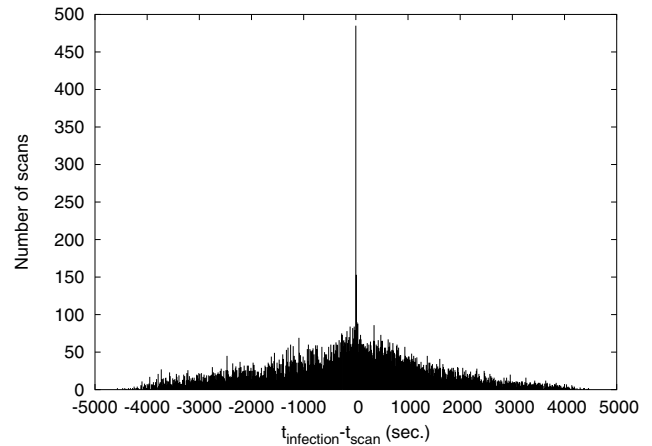Figure 12: Scans from infectees, targeted to other victims.

Figure 13: Number of scans in 10 second buckets.

sponsible for infecting the given target. Negative values mean the target was already infected, while larger positive values imply the scan failed to infect the target for some reason — it was lost,[8] or blocked due to the random destination port it used, or simply the target was not connected to the Internet at that time. (Note that the asymptotic curves at the top and bottom correspond to truncation effects reflecting the upper and lower bounds on infection times.)

The clusters at extreme values of $t_{\text{infection}} - t_{\text{scan}}$ in Figure 12 mask a very sharp additional cluster, even using the log-scaling. This lies in the region $0 < t_{\text{infection}} - t_{\text{scan}} \leq 10$. In Figure 13, we plot the number of scans in 10 second buckets against $t_{\text{infection}} - t_{\text{scan}}$. The very central sharp peak corresponds to the interval 0-to-10 seconds — a clear mark of the dispatch of a successful scan closely followed by the appearance of the victim at the telescope. We plan to continue our investigation of infector-infectee relationships, hoping to produce an extensive "lineage" of infection chains for use in models of worm propagation.

7 Discussion

While we have focused on the Witty worm in this paper, the key idea is much broader. Our analysis demonstrates the potential richness of information embedded in network telescope observations, ready to be revealed if we can frame a precise model of the underlying processes generating the observations. Here we discuss the breadth and limitations of our analysis, and examine general insights beyond the specific instance of the Witty worm.

Candidates for similar analysis. The binary code of all Internet worms is available by definition, making them candidates for disassembly and analysis. Similarly, copies of many scanning and flooding tools have been captured by white hat researchers, and traces observed at telescopes of probing or attack traffic (or backscatter) from the operation of such tools provide candidates for similar analysis. A preliminary assessment we performed of ten well-known DoS attack tools revealed that six of them use simple PRNGs with unsophisticated seeds, while the other four use no random number generation at all. Even with limited knowledge of the operation of such tools, we should in principle be able to analyze logs of their attack traffic or backscatter with a similar intent of reconstructing the sequence of events in the automation of the attack, potentially leading to information about the attacking hosts, their interaction with the network, and other forensic clues.

Diversity of PRNGs. Our analysis was greatly facilitated by the use of a linear congruential PRNG by Witty's author. Reverse-engineering the state of a more complex PRNG could be much more difficult. In the extreme, a worm using a cryptographically strong hash function with a well-chosen key as its PRNG would greatly resist such reverse engineering. However, there are several practical reasons that support the likelihood of many attackers using simpler PRNGs.

Implementing good PRNGs is a complicated task [8], especially when constrained by limits on code size and the difficulty of incorporating linkable libraries. Large-scale worms benefit greatly from as self-contained a design as possible, with few dependencies on platform support, to maximize the set of potential victims. Worms have also proven difficult to fully debug — virtually all large-scale worms have exhibited significant bugs — which likewise argues for keeping components as simple as possible. Historically, worm authors have struggled to implement even the LC PRNG correctly. The initial version of Code Red failed to seed the PRNG with any entropy, leading to all copies of the worm scanning exactly the same sequence of addresses [2]. Slammer's PRNG implementation had three serious errors, one where the author used a value of the parameter b in the LC equation (Eqn. 1) that was larger than the correct value by 1 due to an incorrect 2's complement conversion, another where this value was subtracted from

instead of added to the term aX_i in Eqn 1, and finally the (mis)use of an **OR** instruction rather than **XOR** to clear a key register [11]. In addition, sources of local entropy at hosts are often limited to a few system variables, complicating the task of seeding the PRNG in a fashion strong enough to resist analysis. Thus it is conceivable that worm authors will have difficulty implementing bug-free, compact versions of sophisticated PRNGs.

In addition, today's worm authors have little incentive to implement a complex PRNG. As long as their goals are confined to effectively scanning the IP address space and maximizing the worm's infection rate, simple PRNGs suffice. Hiding one's tracks while releasing a worm can already be accomplished by using a chain of compromised victims as stepping stones. Indeed, the fact that Witty's author left *Patient Zero* running with a separate program for spreading the worm was purely a mistake on his/her part. As discussed earlier, the code it ran scanned a very small subset of the IP address space, and did not manage to produce even one infection during scanning.

Thus, there are significant factors that may lead to the continued use by worms of simple PRNGs such as LC, which, along with the availability of disassembled code, will facilitate the development of structural models of worm behavior to use in conjunction with telescope observations for detailed reconstructions.

General observations from this work. Our study has leveraged the special conditions produced by a worm's release to measure numerous features of its victim population and the network over which it spread. While specific estimation tricks developed in this paper might not apply to other telescope observations in a "cookbook" manner, the insight that telescope observations carry rich information that can be heavily mined armed with a sufficiently detailed model of the underlying source processes is of major significance for the future study of such data.

Understanding the structure of the scanning techniques used by worms (and empirical data on hitherto unmeasured quantities such as distribution of access bandwidth) can be crucial for developing correct models of their spread — a case made for example by our observation of the doubly-scanned and never-scanned portions of the address space, and their multi-factored impact on the worm's growth.

Finally, we would emphasize that the extraction of the features we have assessed was a labor-intensive process. Indeed, for many of them we did not initially apprehend even the possibility of analyzing them. This highlights not only the difficulty of such a forensic undertaking, but also its serendipitous nature. The latter holds promise that observations of other Internet-scale events in the future, even those of significantly different details or nature, will likely remain open to the possibility of such analysis.

8 Conclusions

A worm's propagation is a rare but spectacular event in today's networks. Apart from the obvious disruptions and damage, worms also stress the network in unique ways and at scales unmatched by any controlled measurement experiments. One could say that a worm's release illuminates, for a few moments, dark corners of the network just as supernovae illuminate dark and distant corners of the universe, providing rich observations to telescopes that gather a mere sliver of the enormous radiant flux. But within the overwhelming mass of observed data lies a very structured process that can be deciphered and understood — if studied with the correct model.

We have shown how a fine-grained understanding of the exact control flow of a particular worm — especially its seeding and use of a pseudo-random number generator — when coupled with network telescope data enables a detailed reconstruction of nearly the entire chain of events that followed the worm's release. In the process we have unearthed measurements of quantities such as access bandwidth and system up-time that are otherwise unobservable to the "naked eye" of researchers studying systems from afar. These measurements have applicability to a number of modeling and simulation studies, both in particular to worm propagation analysis, and more generally as a source of rarely-available empirical data. Finally, we have demonstrated the forensic power that such analysis can provide, marshalling strong evidence that the Witty worm specifically targeted a US military base and was launched via an IP address corresponding to a European ISP.

Acknowledgments

References

[1] Michael Bailey, Evan Cooke, Farnam Jahanian, Jose Nazario, and David Watson. The Internet motion sensor: A distributed blackhole monitoring system. In *Proc. NDSS*, 2005.

[2] CAIDA. CAIDA Analysis of Code-Red, http://www.caida.org/analysis/security/code-red/.

[3] CERT. CERT Advisory CA-1999-04 Melissa Macro Virus, http://www.cert.org/advisories/CA-1999-04.html.

[4] Evan Cooke, Michael Bailey, Z. Morley Mao, David Watson, Farnam Jahanian, and Danny McPherson. Toward understanding distributed blackhole placement. In *Proc. ACM CCS Workshop on Rapid Malcode (WORM)*, October 2004.

[5] Domas Mituzas. FreeBSD Scalper Worm, http://www.dammit.lt/apache-worm/.

[6] eEye Digital Security. .ida 'Code Red" Worm, http://www.eeye.com/html/Research/Advisories/AL20010717.html.

[7] Mark Eichin and Jon Rochlis. With microscope and tweezers: An analysis of the Internet virus of november 1988. In *Proc. IEEE Symposium on Research in Security and Privacy*, 1989.

[8] Donald E. Knuth. *The Art of Computer Programming, Second Edition*, volume 2, Seminumerical Algorithms. Addison-Wesley, 1981.

[9] K. Kortchinsky. Black Ice worm disassembly. http://www.caida.org/analysis/security/witty/BlackIceWorm.html.

[10] D. Moore, C. Shannon, G. Voelker, and S. Savage. Network telescopes: Technical report. Technical report, Cooperative Association for Internet Data Analysis (CAIDA), July 2004.

[11] David Moore, Vern Paxson, Stefan Savage, Colleen Shannon, Stuart Staniford, and Nicholas Weaver. Inside the Slammer Worm. *IEEE Security & Privacy*, pages 33–39, July/August 2003.

[12] David Moore, Vern Paxson, Stefan Savage, Colleen Shannon, Stuart Staniford, and Nicholas Weaver. The Spread of the Sapphire/Slammer Worm, 2003.

[13] David Moore, Colleen Shannon, and k claffy. Code-Red: a Case Study on the Spread and Victims of an Internet Worm. In *Proceedings of the Second Internet Measurement Workshop*, pages 273–284, November 2002.

[14] David Moore, Geoffrey M. Voelker, and Stefan Savage. Inferring Internet Denial-of-Service Activity. In *Proceedings of the 10th USENIX Security Symposium*, pages 9–22. USENIX, August 2001.

[15] Ruoming Pang, Vinod Yegneswaran, Paul Barford, Vern Paxson, and Larry Peterson. Characteristics of Internet background radiation. In *Proc. ACM Internet Measurement Conference*, October 2004.

[16] F secure Inc. Global slapper worm information center, http://www.f-secure.com/slapper/.

[17] C. Shannon and D. Moore. The caida dataset on the witty worm, March 19-24 2004. http://www.caida.org/passive/witty/.

[18] C. Shannon and D. Moore. The spread of the Witty worm. *IEEE Security and Privacy*, 2(4):46–50, August 2004.

[19] Eugene Spafford. The Internet worm program: An analysis. purdue technical report csd-tr-823, 1988.

[20] Stuart Staniford and Vern Paxson and Nicholas Weaver. How to 0wn the Internet in Your Spare Time. In *Proceedings of the 11th USENIX Security Symposium*. USENIX, August 2002.

[21] Nicholas Weaver and Dan Ellis. Reflections on Witty: Analyzing the attacker. *;login:*, pages 34–37, June 2004.

[22] V. Yegneswaran, P. Barford, and D. Plonka. On the design and utility of Internet sinks for network abuse monitoring. In *Proc. of Symposium on Recent Advances in Intrusion Detection*, September 2004.

[23] Cliff Changchun Zou, Weibo Gong, and Don Towsley. Code Red Worm Propagation Modeling and Analysis. In *Proceedings of the ACM CCS 2002 conference*, November 2002.

Notes

[1] [21] analyzes what Witty's design implies about its author.

[2] The main body of the Witty worm, including the initial pad required to cause the buffer overflow, fits in 675 bytes. However, the worm picks a larger packet-size, as shown in line 5 of Fig. 2, and pads the tail of the packet with whatever is on the stack, presumably to complicate the use of static filtering to block the contagion.

[3] Since $m = 2^{32}$, the modulo operation is implemented implicitly by the use of 32 bit registers and disregarding their overflow during arithmetic operations.

[4] The only related case of which we are aware was the Melissa email virus [3], where the author posted the virus to USENET as a means of initially spreading his malcode, and was traced via USENET headers.

[5] We ignore infectees that contributed < 20 packets.

[6] We can attribute the missing 5 Mbps to other, ever-present "background radiation" that is a constant feature at such telescopes [15].

[7] The distortion is not static but evolves with the spread of the worm. By tracking changes in the slope of the upper envelope, we can infer the value of the distortion against time throughout the period of activity of the worm.

[8] Recall that the effective bandwidth of most infectees is much lower than the access bandwidth, indicating heavy loss in their generated traffic.